JOURNAL OF COMPUTATIONAL PHYSICS 31, 301–312 (1979)

Pitch Angle Diffusion of Trapped Particles in the Presence of a Loss Cone: Calculating the Distribution of Particles Precipitating from the Earth's Radiation Belts

G. T. DAVIDSON

Lockheed Palo Alto Research Laboratory, 3251 Hanover Street, Palo Alto, California 94304

Received October 28, 1977; revised August 18, 1978

The distribution of stably trapped particles in a magnetic mirror field evolves according to a Fokker-Planck diffusion equation in phase space. In the earth's trapped radiation belts this diffusion equation has usually been averaged over the field lines. The correct treatment of the loss cones demands a detailed integration along the field lines. A method is described here for integrating the pitch angle diffusion equation by finite difference techniques. The pitch angle variable is replaced by an adiabatic invariant variable, and a triangular coordinate grid is constructed for the finite differences. The integration can be iterated back and forth along the field lines until convergence is established. Results are presented for trapped protons. Applications to the scattering of electrons in the atmosphere are discussed.

1. INTRODUCTION

The earth's trapped radiation belts constitute a well known example of stable confinement of charged particles in a magnetic mirror geometry. The most important loss processes are particle collisions and wave-particle interactions, which result in pitch-angle diffusion, followed by escape or absorption at the mirror ends.

The analytical methods used for treating the radiation belt particles have generally been similar to those applied to laboratory mirror machines. There are, however, differences in scale, geometry, and diagnostic techniques that demand different approaches to diffusion into the loss cone. The first approximation in both cases has been the bounce-average Fokker–Planck equation, which is valid for the majority of the particles [1, 2, 3, 4]. The bounce-averaged FP equation is not adequate to describe the details of the distribution in and near the loss cones [4, 5]. In the following Section 2, I will briefly discuss the limitations of bounce-averaging, and the methods that have been previously employed to overcome those limitations. In Section 3, I will present an alternate method for integrating the complete FP equation in the trapped radiation belts. The new method is based on an adiabatic invariant formulation of the basic equations, and employs finite-difference techniques. In the last Section 4, I will discuss some possible applications to related problems.

An earlier paper has been published on the physical principles and results for radiation belt electrons [6]; that paper will hereafter be referred to as Paper I. The

0021-9991/79/060301-12$02.00/0

calculations described here apply mainly to trapped protons which are conceptually easier to understand because the protons are not backscattered from the mirror ends, allowing a pure absorption boundary condition.

2. The Pitch-Angle Diffusion Equation

2.1. *The General Form of the Fokker–Planck Diffusion Equation*

The Fokker–Planck equation for radiation belt particles can generally be reduced to a diffusion-type equation of the form [1, 2, 3, 7]

$$\begin{aligned}\frac{df}{dt} &= \frac{\partial f}{\partial t} + \bar{V}\cdot\nabla f \\ &= \frac{1}{\sin\alpha}\frac{\partial}{\partial\alpha}\left[D_{\alpha\alpha}\sin\alpha\frac{\partial f}{\partial\alpha}\right] \\ &\quad - \{\text{energy loss}\} + \{\text{sources}\} - \{\text{losses}\}\end{aligned}$$

where $f(t, s, E, \alpha)$ is the phase space number-density distribution function and $D_{\alpha\alpha}(t, s, E, \alpha)$ is the pitch angle diffusion coefficient. The independent variables are time t, distance along a field line s, energy E, and pitch angle α (defined as the angle between the momentum vector and field line); V is the velocity. The energy loss term is important for collisions with particles [1], but can usually be ignored for wave-particle interactions in the radiation belts [2, 8]. In the following discussion I will concentrate on the pitch angle diffusion and ignore the last three { } terms.

The proper independent variable on the right side of Eq. (1) should depend only on the first adiabatic invariant [9]. An advantageous choice is (ignoring the dependence on E)

$$u \equiv 1 - \frac{B_0}{B}\sin^2\alpha \tag{2}$$

where B_0 is the minimum magnetic field strength—or equatorial field—and $B = B(s)$ is the local field. Defined this way u is a local variable that becomes equal to $\cos^2\alpha_0$ at the equator. The FP equation can now be written

$$\begin{aligned}&\frac{\partial f}{\partial t} + \frac{V}{R_0}\left(1-(1-u)\frac{B}{B_0}\right)^{1/2}\frac{\partial f}{\partial s} \\ &\quad = 4\frac{B_0}{B}\left(1-(1-u)\frac{B}{B_0}\right)^{1/2}\frac{\partial}{\partial u}\left[D_{\alpha\alpha}\left(1-(1-u)\frac{B}{B_0}\right)^{1/2}(1-u)\frac{\partial f}{\partial u}\right].\end{aligned} \tag{3}$$

The distance s is in units of a dimensional parameter R_0; in the earth's field $R_0 = L \cdot$ (earth's radius) is the radial distance to the equatorial crossing.

2.2. *Limits on the Validity of the Bounce-Averaged Diffusion Equation*

If the distribution function is sufficiently uniform along the field lines, the bounce-averaged diffusion equation follows immediately upon an integration of Eq. (3) with respect to $ds/\cos\alpha$. For particles outside the loss cone $\alpha_0 < \alpha_c$ (1, 2)

$$\frac{\partial f}{\partial t} \simeq \frac{1}{\tau_B}\frac{\partial}{\partial u_0}\left[\langle D_{u_0u_0}\rangle \tau_B \frac{\partial f}{\partial u_0}\right] \tag{4a}$$

$$\langle D_{u_0u_0}\rangle = \frac{4R_0}{V\tau_B}\oint D_{\alpha\alpha}(1-u_0)\frac{B_0}{B}\left(1-(1-u_0)\frac{B}{B_0}\right)^{1/2} \tag{4b}$$

where τ_B is the bounce period and $u_0 = \cos^2\alpha_0$ is evaluated at the equator.

For weak diffusion the diffusion or collision time τ_L is $\gg\tau_B$, and the assumption that f is independent of s breaks down near and inside the loss cone. The number of particles in the loss cone increases monotonically with s from one mirror end to the other [5]. Several approximations have been introduced to treat the loss cones in the radiation belts. Simply ignoring the $\partial f/\partial s$ term and introducing large values of $D_{\alpha\alpha}$ for collisions with atmospheric particles gives nearly correct loss rates [1, 7, 10], but does not preserve the details of the loss cone distribution. One can, alternatively, integrate the $\partial f/\partial s$ term between two mirror points, s_1 and s_2, within the atmosphere to obtain a finite term of order $2(f_2 - f_1)/\tau_B \approx 2f/\tau_B$. In practice this approximation has been used with the equatorial distribution function $f(t, u_0) \equiv f(t, \cos^2\alpha_0)$ and an ad hoc multiplication factor $w \approx 2$. The resulting equation for the loss cone is similar to Eq. (4), but with an atmospheric loss term $-2wf/\tau_B$ on the right side [11, 12, 13]. The weakness of this approach is that $f(t, u_0)$ does not truly repreesnt a phase space distribution function but rather $F(t, u_0)/(\tau_B(u_0)^{1/2})$, where F is the total distribution function for all the particles contained within a tube of field lines [1]. The linear loss term is of little use when appreciable numbers of particles are backscattered from the atmosphere [6].

An approach that has proved useful for treating the spatially dependent distribution function in laboratory mirror machines is an expansion based on the scaling ratio $\lambda = \tau_B/\tau_L$ [5]. The expansion method does not seem to be readily applicable to the highly inhomogeneous radiation belts where the diffusive interactions may be concentrated both near the central plane (equator) and at the mirror ends [1, 2]. The scaling ratio λ is usually extremely small for radiation belt particles mirroring above the atmosphere, but increases rapidly as the mirror points dip into the atmosphere, approaching a value of unity. The particles that just skim the top of the atmosphere may make many bounces before they are lost [1], thereby violating one of the principal assumptions of the expansion, namely that diffusion at the mirror ends is negligible [5].

The solutions of the bounce averaged diffusion equation are of interest here because they provide a useful starting point for an iterative solution of the FP equation. They also provide a basis for comparisons with the correct spatially dependent solutions. Consider a steady state for which $\partial f/\partial t = 0$.

Simple solutions can be found for a diffusion coefficient of the form

$$\langle D_{u_0 u_0} \rangle = D \frac{8(1 - u_0)}{\tau_B} \sin^2 \alpha_c \tag{5}$$

where D is a dimensionless constant. If the source that maintains the particles vanishes in the loss cone, the solution there is [11]

$$f \propto \left(\frac{D}{w}\right)^{1/2} I_0 \left(\left(\frac{w}{D}\right)^{1/2} \frac{\sin \alpha_0}{\sin \alpha_c}\right) \Big/ I_1 \left(\frac{w}{D}\right)^{1/2} \tag{6}$$

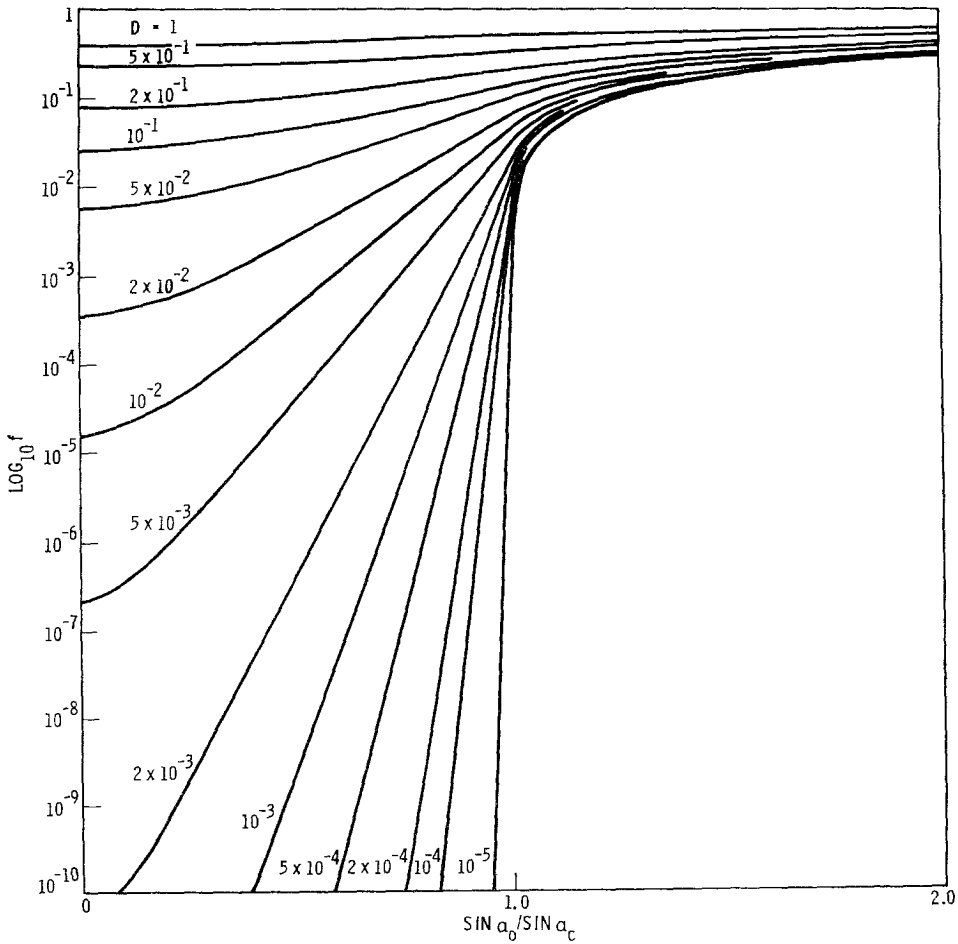

FIG. 1. The bounce-average pitch angle distributions in and near the loss cone. The examples plotted are for 50 keV protons at $L = 4$; for other cases the solutions to the diffusion equation inside the loss cone ($\sin \alpha_0 / \sin \alpha_c = \sin \alpha < 1$) will be shifted upward or downward with slight changes in the shapes of the right-hand portions (trapped) of the curves.

where I_0 and I_1 are Bessel functions of imaginary argument. The loss cone solutions depend on the parameter D/w; the trapped particle solutions beyond α_c depend also on the length of the field line. Solutions of Eq. (4) are plotted in Fig. 1 for 50 keV protons at $L = 4$ and a source proportional to $(\sin^2 \alpha_0 - \sin^2 \alpha_c)/\tau_B = (u_c - u_0)/\tau_B$; w was taken equal to 1.

3. Integration of the Fokker-Planck Equation

Integration of the FP equation (3) poses some novel difficulties, manily because of the distortion of the domain of integration. The domain of integration in the u, s plane is illustrated in Fig. 2 for a dipole field. The transformation from local pitch angle to adiabatic invariant coordinate u has split the domain of integration into two parts, joined along the curve of mirror points, $u = u_m(s)$. The two separate regions are superimposed in Fig. 2, with the mirror point curve on the left. When it is necessary to distinguish the two regions they may be labelled "DOWN" or "UP". (In effect the two regions correspond to particles travelling in opposite directions with local pitch angles $0 \leqslant \alpha \leqslant 90°$ and $90° \leqslant \alpha \leqslant 180°$, respectively.)

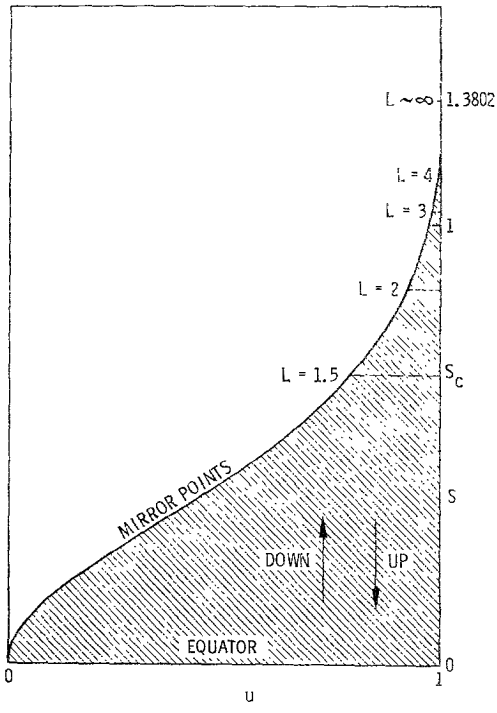

FIG. 2. The domain of integration in the u, s plane. Only the $s \geqslant 0$ half is shown. The location of the intersection with the atmosphere is indicated by horizontal dashed lines at s_c, with the corresponding L value listed to the side.

Equation (3) lends itself readily to finite difference methods for its solution. However, the steep gradients expected in f at the edge of the loss cone necessitate compressing a large number of integration points into the vicinity of $u_m(s) = u_c$ at the atmosphere, $s = s_c$. One way this can be accomplished is by constructing polynomials $P_u(i)$ and $P_s(j)$ to represent the integration variables u and s as functions of the grid point indices, i and j. The errors usually associated with highly non-uniform grids are minimized if the polynominals over adjacent ranges are continuous in their first and second derivatives [14]. Furthermore there are advantages in using the same polynominal to represent both u and s. Let P be a polynominal in i or j, and

$$P_i \equiv u_i = 1 - \frac{B_0}{B}\sin^2\alpha \tag{7a}$$

$$P_j \equiv 1 - \frac{B_0}{B(s_j)}. \tag{7b}$$

The FP equation for a steady state, $\partial f/\partial t \equiv 0$, then becomes a finite difference equation,

$$\frac{\delta f}{\delta j} = \frac{\delta}{\delta i}\left[D_{\alpha\alpha}\frac{4R_0}{V}\left(\frac{B_0}{dB(s_j)/ds_j}\right)\frac{(1-P_j)}{(1-P_j)}\left(1-\frac{(1-P_i)}{(1-P_j)}\right)^{1/2}\frac{P_j'}{(P_i')^2}\frac{\delta f}{\delta i}\right] + \{\text{sources}\}$$

$$= \frac{\delta}{\delta i}\left[\mathscr{D}_{ij}\frac{\delta f}{\delta i}\right] + \{\text{sources}\} \tag{8}$$

where P_j' is the customary notation for a derivative evaluated at i. The extension to non-equilibrium cases is straightforward, though special care would be needed to achieve adequate time steps without excessive computation time. The mirror points now fall on the diagonal line $i = j$; each j row contains one less (or more) point than the adjacent row.

The matrix form of the implicit difference equations is obtained by finding the averages of $\delta f/\delta j$ over each box of four points (i,j), $(i,j+1)$, $(i+1,j+1)$, $(i+1,j)$, and multiplying by $\mathscr{D}_{i+1/2,j+1/2}$ evaluated in the center of the box. This scheme has the advantage that the same coefficients appear in the difference equations for the DOWN and UP integrations. The finite difference equation for both DOWN and UP can be formulated for the increments $\Delta_i = f_{i,j_2} - f_{i,j_1}$ between the rows j and $j+1$, thus

$$-C^j_{i,i-1}\Delta_{i-1} + (1 - C^j_{i,i})\Delta_i - C^j_{i,i+1}\Delta_{i+1}$$

$$= 2C^j_{i,i-1}f_{i-1} + 2C^j_{ii}f_i + 2C^j_{i,i+1}f_{i+1} \tag{9a}$$

$$C^j_{i,i-1} = 1/2\mathscr{D}_{i-1,j+1/2} \tag{9b}$$

$$C^j_{i,i+1} = 1/2\mathscr{D}_{i+1,j+1/2} \tag{9c}$$

$$C^j_i = -C^j_{i,i-1} - C^j_{i,i+1}. \tag{9d}$$

At the line $i = j$, $\mathscr{D}_{ij}$ vanishes so the difference equation for the trapezoidal box

bounded by the points (j,j), $(j+1,j+1)$, $(j+2,j+1)$ and $(j+2,j)$ does not contain the expected term with f_{jj}:

$$(1 - C^j_{j+1,j+1})\,\Delta_{j+1} - C^j_{j+1,j+2}\Delta_{j+2} = 2C^j_{j+1,j+1} + 2C_{j+1,j+2}f_{j+2} \tag{10a}$$

$$C^j_{j+1,j+2} = -C^j_{j+1,j+1} = 1/2D_{j+3/2,j+1/2}\,. \tag{10b}$$

The right and left halves of the grid in Fig. 3 are thereby effectively disconnected. Ordinarily one would expect that a step from one j line to the next would involve transfers of particles across the mirror point curve—from local pitch angles less than 90° (right half of grid) to local pitch angles greater than 90° (left half of grid), and vice-versa. However, a peculiar property of the FP equation (3) for small angle scattering is that the current (the [ ] bracketed term) across $\alpha = 90°$ is zero—there is a net balance of particles being deflected toward either direction. The integration is split into two sets of difference equations, coupled only through the atmospheric boundary condition and the identity of DOWN and UP fluxes on the line of mirror points.

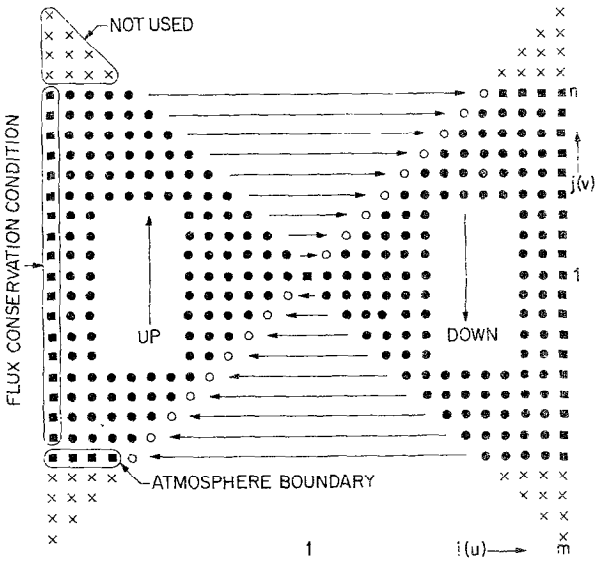

FIG. 3. The finite-difference integration grid. The points at which the distribution function is to be evaluated are denoted by solid circles. The boundary conditions are applied at the points denoted by solid squares. The indices i and j are presumed equal to 1 in the center and increase toward the outer edges.

Integrations were carried out by stepping forward from one j line to the next using only half the points along each line (e.g., DOWN). On reaching the atmosphere at $j = n$, the direction of integration was reversed to fill in the opposite side of the grid (e.g., UP). The reverse integration picked up an additional grid point j, j at each step, along with the last previously computed value of f_{jj} (open circles in Fig. 3). The iterative procedure is equivalent to an integration with periodic boundary conditions;

and was continued in a clockwise direction around Fig. 3 until satisfactory convergence was attained.

The unknown values of f were calculated at the interior points (solid circles) of the grid. The total number of unknowns is $2[(m-n)(m+n-1)+(n-1)]+1$. Boundary conditions were specified along the lines $j=n$ (atmosphere) and $i=m$. For trapped protons the atmospheric boundaries were regarded as perfect absorbers at an altitude of 100 to 120 km [15, 16]. Whenever backscatter from the atmosphere becomes important, as in the case of trapped electrons, it is necessary to continue the integration down through the atmosphere, using a diffusion coefficient $D_{\alpha\alpha}$ appropriate to particle collisions, and including an energy loss term [6, 17]. Conservation of current (the [ ] term in Eq. (8)) leads to a derivative boundary condition:

$$(1-P_i)\left(\frac{\delta f_i}{\delta P_i}\right)_{i=m} = \left[\frac{\delta f_i}{\delta \ln(1-P_i)}\right]_{i=m} = 0$$

$$\propto (f_{m-2}-f_m)(1-P_{1-m})^2-(f_{m-1}-f_m)(1-P_{m-2})^2. \quad (11)$$

The difference equations plus these boundary conditions leaves one fewer equations than unknowns. An obvious place to specify the remaining condition is at the center point, $i=j=1$. In a completely symmetric grid a derivative condition $\partial f/\partial m=0$ is useful.

3.2. *Numerical Integration and Results*

The results of the numerical integration of Eq. (8) are sensitive to the values of $D_{\alpha\alpha}$ and to the boundary condition at s_c. The value of $D_{\alpha\alpha}$ is, however, largely unknown. For small loss cones ($L>2$) the results are expected to be more sensitive to the magnitude than to the form of $D_{\alpha\alpha}$. For the sample calculations I assumed the average values given by Eq. (5), and let $D_{\alpha\alpha}$ be a function solely of u. The approximate values of $D_{\alpha\alpha}$ are (18).

$$D_{\alpha\alpha} = D\frac{V\sin^2\alpha_c}{2R_0Z} \quad (12a)$$

$$Z \equiv 1/4\oint \frac{B_0}{B}\cos\alpha\, ds$$

$$\simeq .4575u + .2326(1-u)[1-(1-u)^{3/8}]. \quad (12b)$$

Ideally it would be desirable to have an integration grid that optimizes the values of the finite difference coefficients. For computational efficiency the C_{ii}^j's should be near their stability limit [19].

$$C_{ii}^j > -1. \quad (13)$$

It is apparent that such an optimum computational grid for very small values of D would be impractically large. The difficulty is rooted in the extreme smallness of the ratio of τ_B (seconds) and τ_L (up to months of years). The integration grid was therefore optimized around the cutoff, u_c; using third degree polynomials to represent u_i in

the loss cone and fourth or fifth degree polynomials for $i < n$. Solutions of Eq. (4) were used to start with a very accurate approximation over most of the range of u and s. Symmetry about the equator was assumed in the sample cases, and the computation was merely stopped and turned around at $j = 1$. After a few iterations (<20) quite satisfactory solutions were obtained in and near the loss cone. With the partially optimized grids the number of points needed to describe the loss cone portion of the distribution increased approximately with $\log(D)$, from 8×8 points at $D \simeq .1$ to 40×40 points at $D \simeq 10^{-4}$.

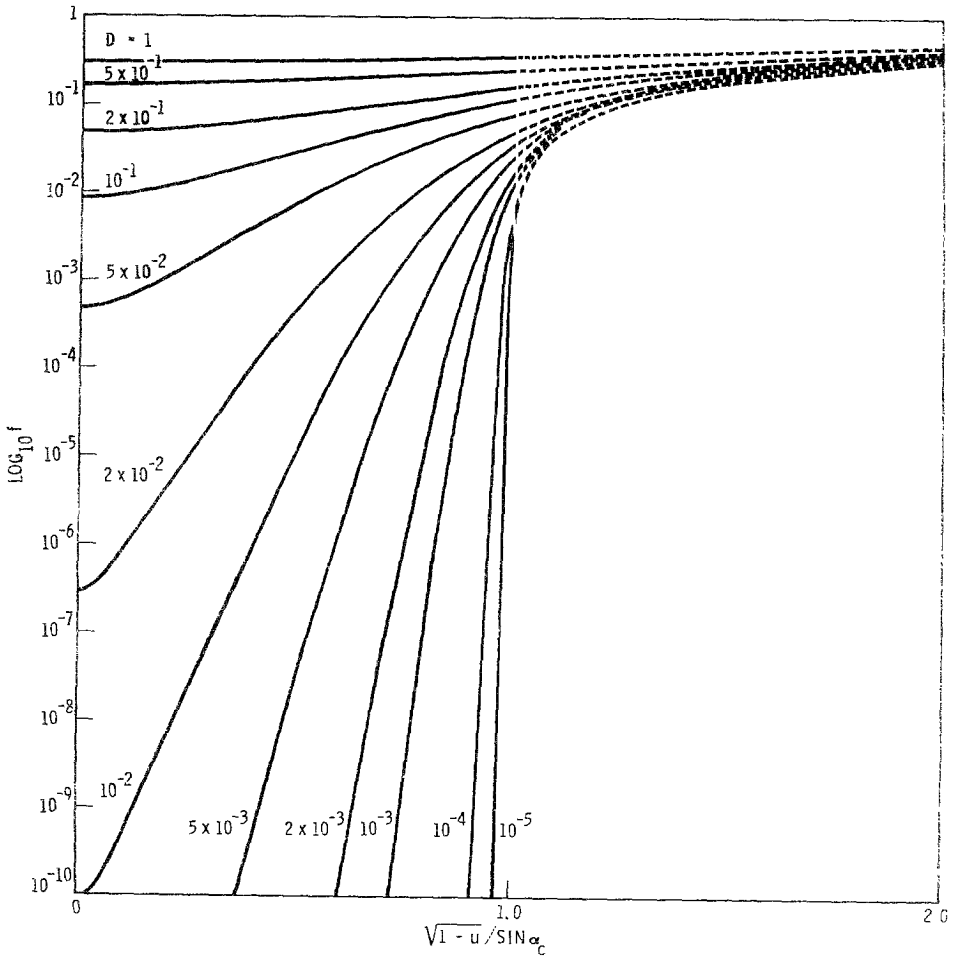

FIG. 4. Sample computed distributions of 50 keV protons at $L = 4$ as they would be observed immediately above the atmosphere. The diffusion coefficients (defined in the text) yield the same bounce-averaged diffusion coefficients as applied to Figure 1. The left half of the figure is the local pitch-angle distribution at the top of the atmosphere, up to sin $(90_a) = 1$. The dashed curves on the right are the phase space densities of locally mirroring particles at $B = B_0/(1 - u)$.

A realistic choice of a source distribution is one whose strength falls off rapidly from $\alpha = 90°$ toward the loss cones, and which is concentrated near the equator. With these limitations the results for the loss cone distribution are insensitive to the details of the source. An adequate representation was found to be a source that only entered the calculation at the equator ($j = 1$), with a pitch angle dependence $(u_c - u_i)$, similar to that of Fig. 1.

Figure 4 shows the results of sample calculations for 50 keV protons entering the atmosphere at $L = 4$. The cases illustrated correspond to the same set of diffusion coefficients as in Fig. 1. The abscissa from 0 to 1 is equivalent to the sine of the local pitch angle. Properly the local distributions should be cut off at $\sin \alpha = 1$, but the loss cone distributions here have been joined to the phase space densities of locally mirroring protons at $B = B_0/(1-u_0)$. This provides an unambiguous definition of the trapped distribution, and is equivalent to the definition of the bounce averaged $F(t, u_0)$. The trapped distributions on the right side of the figure are nearly identical with the bounce-averaged values of Fig. 1.

Trial calculations at L values other than 4 gave similar results in the loss cone. Depending on the D value, a grid of less than 100×100 points was adequate for all of the trial cases. The number of iterations necessary to achieve a satisfactory result depends on the grid, the type of boundary condition at the atmosphere, and the accuracy of the initial approximations. Test cases were run to as many as 60 iterations without evidence of instabilities, though a smaller number is probably adequate for any realistic problem. A complete integration could be run on a medium capability computer (CDC 6600/IBM 360/Univac 1110) in 1 to 10 minutes. The running time is, of course, longer for the electron case, where diffusion and energy loss in the atmosphere must be taken into account.

4. Discussion and Conclusions

It was no surprise that the loss cone distributions of Figs. 1 and 4 bear a superficial resemblance to one another, even though they represent different aspects of the distribution function. Properly, Fig. 1 should must nearly represent the distribution in the equatorial plane. Close agreement with the true distribution at the top of the atmosphere can be achieved by adjusting the loss rates in the bounce-averaged equation by a factor $w \approx 2$, though such a consideration does not seem to have entered the reasoning behind the original derivation of the loss term [11, 12, 13]. The bounce-averaged method, which is much simpler to execute, can therefore be used with good chances of success in restricted types of problems. But, when detailed pitch-angle and spatial distributions are desired in the loss cone, the complete FP equation must be solved.

That the detailed solutions for the cases discussed here resemble the bounce-averaged solutions leads us to suspect that, for suitable cases, the bounce averaged equation might be of use for electrons in the loss cone. The factor w might then be

approximated by an empirical function of energy and pitch-angle. The values of w would have to be derived from the results of detailed integrations.

The most notable feature of the calculations described here is the utilization of the vanishing current in the FP equation at local pitch angles of 90°. This made possible the separation of DOWN and UP integrations and a consequent improvement in the efficiency of the computer codes. Similar methods, taking advantage of the converging field and particle mirroring, should also be applicable to the penetration of energetic particles into the atmosphere. Several computer codes have been developed to treat electron scattering in the atmosphere [16, 20, 21], including the one employed in the trapped electron calculations of Paper I [6]. Apparently none of the existing electron scattering codes employs an explicitly adiabatic-invariant formulation. This may reduce their ability to treat mirroring effects and to handle pitch angle distributions with sharp gradients near 90° pitch-angles. An adiabatic invariant method is directly applicable, and might alleviate some of the computational difficulties encountered in the atmospheric scattering codes. The methods described above could also reduce (or eliminate) the need for iterations of the spatial integration.

ACKNOWLEDGMENTS

I wish to thank especially M. Walt, G. E. Crane, J. B. Cladis, and M. Schulz for many stimulating discussions and helpful suggestions. I would also like to thank one of the referees for bringing to my attention an important related paper. The work described here was supported by DNA contract 001-76-C-0247 and by Lockheed independent research funds.

REFERENCES

1. W. M. MACDONALD AND M. WALT, *Ann. Phys. (N.Y.)* **15** (1961), 44.
2. L. R. LYONS, R. M. THORNE, AND C. F. KENNEL, *J. Geophys. Res.* **77** (1972), 3455.
3. J. KILLEEN AND K. D. MARX, *in* "Methods in Computational Physics" (B. Alder, S. Fernbac, and M. Rotenberg, Eds.), p. 421, Academic Press, New York, 1970.
4. D. J. BENDANIEL AND W. P. ALLIS, *Plasma Phys.* **4** (1962), 31.
5. D. E. BALDWIN, J. G. CORDEY, AND C. J. H. WATSON, *Nuclear Fusion* **12** (1972), 307.
6. G. DAVIDSON AND M. WALT, *J. Geophys. Res.* **82** (1977), 48.
7. M. WALT AND W. M. MACDONALD, *J. Geophys. Res.* **67** (1962), 5013.
8. C. F. KENNEL AND H. E. PETSCHEK, *J. Geophys. Res.* **71** (1966), 1.
9. T. G. NORTHROP, "The Adiabatic Motion of Charged Particles," Interscience, New York, 1963.
10. W. N. SPJELDVIK AND R. M. THORNE, *J. Atmos. Terr. Phys.* **37** (1975), 777.
11. C. F. KENNEL, *Rev. Geophys. Space Phys.* **7** (1969), 379.
12. G. C. THEODORIDIS AND F. R. PAOLINI, *Ann. Geophys.* **23** (1967), 375.
13. T. A. FRITZ, *in* "Magnetospheric Physics" (B. M. McCormac, Ed.), p. 105, Reidel, Dordrecht, Netherlands, 1974.
14. E. K. DE RIVAS, *J. Computational Physics* **10** (1972), 202.
15. A. M. LENCHEK AND S. F. SINGER, *Planet. Space Sci.* **11** (1963), 1151.
16. M. WALT AND W. M. MACDONALD, *Rev. Geophys.* **2** (1964), 543.
17. M. WALT, W. M. MACDONALD AND W. E. FRANCIS, *in* "Physics of the Magnetosphere" (R. L. Carovillano, Ed.), p. 534, Reidel, Dordrecht, Holland, 1969.

18. M. SCHULZ, *J. Geophys. Res.* **81** (1976), 5212.
19. G. F. FORSYTH AND W. R. WASOW, "Finite Difference Methods for Partial Differential Equations," Wiley, New York, 1960.
20. D. J. STRICKLAND AND L. B. BERSTEIN, *J. Appl. Phys.* **47** (1976), 2148.
21. D. J. STRICKLAND, D. L. BOOK, T. P. COFFEY, AND J. A. FEDDER, *J. Geophys. Res.* **81** (1976), 2755.